Formation of Aluminium Carbide in Hall-Héroult Electrolysis Cell Environments

Bronislav NOVAK[1], Arne P. RATVIK[2] (arne.p.ratvik@sintef.no, +4792296156), Zhaohui WANG[2] (zhaohui.wang@sintef.no, +4746249405), and Tor GRANDE[1] (grande@ntnu.no, +4797616918)
[1]Department of Materials Science and Engineering, Norwegian University of Science and Technology, NO-7491 Trondheim, Norway
[2]SINTEF Materials and Chemistry, NO-7465 Trondheim, Norway
[3]Corresponding author: grande@ntnu.no

Keywords: aluminium carbide, cathode wear, aluminium reduction

Abstract

The formation and dissolution of aluminium carbide under conditions similar to the chemical and electrochemical environments in the Hall-Héroult process were studied in laboratory cells, including cells with reversed polarization. The cross sections of the various electrochemical cells after the electrolysis experiments were characterized by optical and electron microscopy. A relatively dense layer of aluminium carbide was observed on the carbon cathode surface under conventional electrolysis conditions. Aluminium carbide was also found in the pores of the cathode together with bath, while only bath was found in the anode. While the direct chemical reaction between carbon and aluminium to form Al_4C_3 is slow, the polarisation of the cathode and electrolysis were demonstrated to have a pronounced effect on the formation of Al_4C_3. The present finding is discussed with emphasis of the difference between chemical and electrochemical formation of Al_4C_3 and the importance of the initial presence of aluminium at the cathode.

1   INTRODUCTION

The most common reason for the shutdown of aluminium electrolysis cells is the degradation of the cathode lining. The lifetime of the cathode is mainly determined by cathode wear, where the current density has been shown to be the most influencing factor [1-3]. The cathode wear mechanism has received increasing attention because aluminium producers have shifted towards cells with higher amperages, which has resulted in a shift towards graphitized cathodes with higher electrical conductivity. Pure mechanical wear due to movement of the aluminium pad has been addressed, but most likely is the wear mechanism related to the formation of aluminium carbide, which can be formed either chemically or electrochemically and transported away from the cathode by dissolution into the bath. Despite the importance of the cathode wear phenomenon, the mechanism(s) of cathode wear and aluminium carbide formation are not clearly understood [1-3].

The first study of the interaction between aluminium and carbon was reported by Dorward [4]. Aluminium did not wet carbon, and the wetting angle was approaching 180°. When a film of cryolite was introduced, the wetting was strongly enhanced to almost 0° and the layer of aluminium carbide was formed on the carbon surface. The formation of a dense layer of aluminium carbide was used to explain the improved wetting. The formation of aluminium carbide has recently been studied by aluminium-carbon diffusion couple experiments by the present authors [5, 6]. Aluminium does not wet carbon and the surface of aluminium is covered by a thin protective layer of aluminium oxide [7]. This layer can be removed and aluminium carbide can be formed at temperatures higher than 1100 ℃. The vapor pressure of aluminium suboxide in Reaction 1 reaches $\sim10^{-6}$ bar at 1100 ℃, which allows the evaporation of the thin oxide layer at atmospheric conditions.

$$Al_2O_3(s) + 4Al(l) \rightarrow 3Al_2O(g) \qquad (1)$$
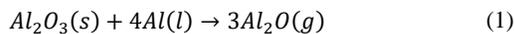
Aluminium carbide was observable at the interface already after one day and compact bilayers were developed after ten days. The first, thinner layer towards aluminium had higher oxygen content than the second, thicker layer towards carbon that was almost pure aluminium carbide [5].

A gas transport mechanism was also suggested as a possible mechanism, where Al_2O gas may transport Al towards the carbon surface by Reaction 2 and CO transports C to the aluminium surface by Reaction 3 [5].

$$2Al_2O(g) + 5C(s) = Al_4C_3(s) + 2CO(g) \qquad (2)$$

$$\frac{1}{2}CO(g) + Al(l) = \frac{1}{6}Al_4C_3(s) + \frac{1}{6}Al_2O_3(s) \qquad (3)$$
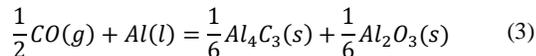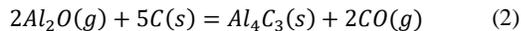
When a film of cryolite was introduced at the carbon aluminium interface, aluminium carbide was found already after 3 hours [6]. The small amount of cryolite did however evaporate relatively fast due to the high volatility in presence of aluminium, and a textured layer of carbide needles was found towards the aluminium surface. A thin layer of aluminium carbide was found towards carbon in line with previous reports.

Grjotheim studied formation of aluminium carbide formation in the vicinity of cryolite without any electrolysis reaction taking place [8]. The reaction was shown to proceed until saturation, and the layer of carbide was suggested to be formed at the carbon surface. In aluminium electrolysis cell the strong correlation between local current density and the wear rate has recently been reported [9]. In laboratory test cells, the wear rate is rising parabolically with current density and reaches an asymptotic value [3, 10]. The process may be limited by aluminium

carbide dissolution into the bath and mass transfer. The hydrodynamics around the cathode surface was shown to be very important [11] and is often considered as the rate determining step.

In the present work, the influence of cryolite without polarisation or electrolysis was investigated with cells corresponding to the conventional set-up with bottom cathodes and inverted electrochemical cells with cathodes at the top. The aim was to investigate the difference between chemical and electrochemical formation of aluminium carbide.

2   EXPERIMENTAL

The influence of polarisation and electrical current on the formation of aluminium carbide was studied in electrochemical cells illustrated in Fig. 1. Experiments without polarisation were conducted in a carbon crucible similar to previously used in diffusion couple experiments [5, 6]. Electrochemical cells have alumina linings with a circular hole in the bottom for the electrodes connected to a carbon platform connection. Fully graphitized carbon IG-15 (Toyo Tanso, graphitization at 3000 °C with bulk density 1.9 g/cm^3) was used because of its high degree of graphitization. The aluminium cylinder was made of aluminium with high purity (99.99 %). The bath consisted of synthetic cryolite (Sigma-Aldrich) and 20 wt% (40 at%) addition of calcium fluoride (Alfa Aesar) to reduce the melting point and the vapor pressure of the electrolyte. 5 % of alumina (Merck) was added to the electrolyte to promote the electrolysis reaction.
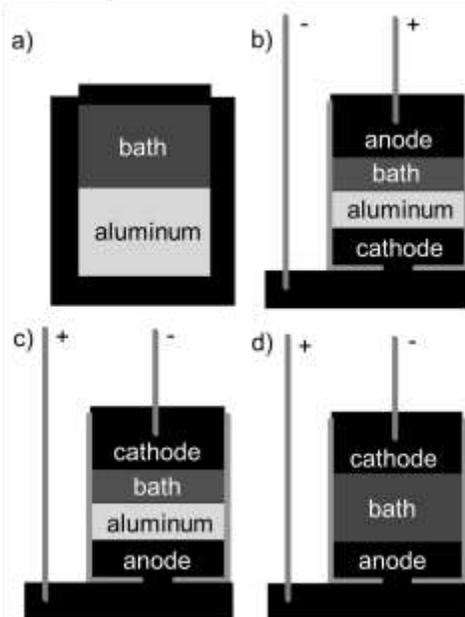
Fig. 1   Test configurations: a) reference experiment without current, b) conventional cell, c) inverted cell, d) inverted cell without aluminium

The cell was placed into a fused silica-liner as illustrated in Fig. 2. The liner was evacuated down to 2 mbar and re-filled with Ar gas (Yara Praxair 5.0) to 0.3 bar to reach less than 1 bar at electrolysis temperature at 980 °C (preheated to 1020 °C for 3.5 hours). A Hewlett Packard power supply was used and the cell voltage and current was recorded. The duration of electrolysis was from 0.5 to 3 hours at a constant current of 0.2 A/cm^2. The experiments without polarisation were conducted from 3 hours to 3 days.
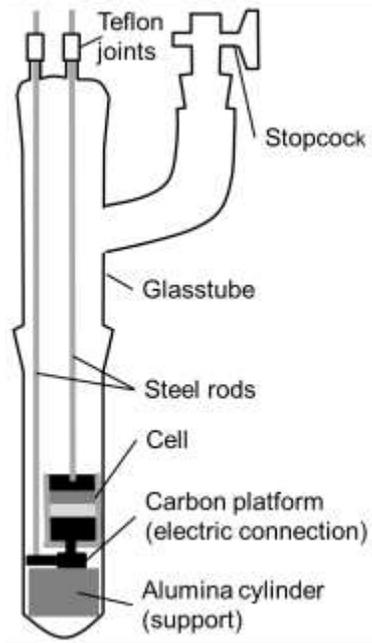
Fig. 2   Schematic drawing of the experimental setup of electrolysis (not in scale)

After the experiment the cells was embedded in epoxy resin and cut into two. The cross section was polished to 0.25 μm, using 100 % ethanol as lubricant. The cross-section was analysed by optical microscope, scanning electron microscopy and element mapping using LV-SEM HITACHI S-3500N with energy dispersive spectroscopy (EDS).

3   RESULTS

3.1   Experiments without polarisation

Experiments without polarisation were performed as a reference with purely chemical interaction between C and Al. An optical image of the bottom of the cell together with element distribution is shown in Fig. 3. A gap between the bath and aluminium was formed during cooling, making the interface between the bath and aluminium challenging to analyse. No aluminium carbide was observed at the carbon-aluminium interface after 3 hours. The five element maps support the conclusion that no carbide layer is formed. The bath has also penetrated into the pores of the carbon material, which is also evident from the Al, Na and F element maps.
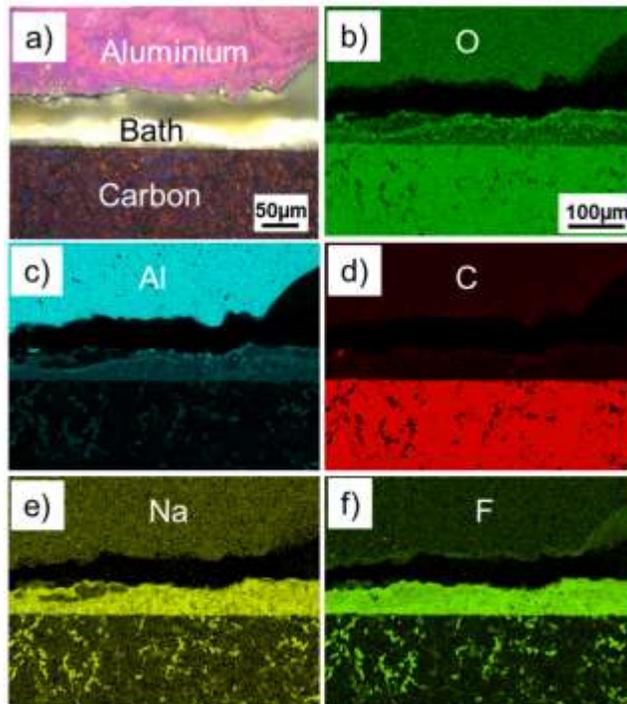
Fig. 3   Al/C interface without polarisation at 980 °C for 3 hours. a) polarised light image. b-f) O, Al, C, Na and F element maps

Optical images of the carbon crucible after 3 days at 980 °C without polarisation are shown in Fig. 4. A layer of aluminium carbide has formed towards the carbon surface, evidenced by the typical pink/purple colour using polarised light. The morphology of carbide layer reflects the topography of the carbon. Figure 3b demonstrates that the carbide layer is porous and that the pores are filled with bath. In some regions (Figure 4c), a delaminated carbide layer is followed by the formation of a new layer.
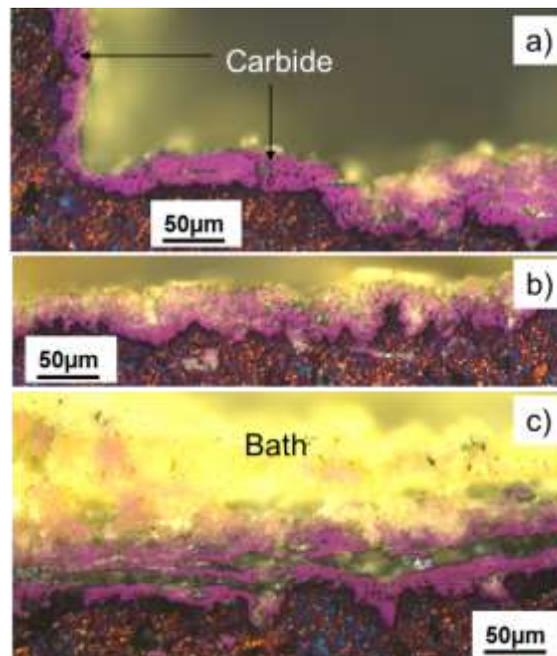
Fig. 4   Optical images of the aluminium carbide layer on the carbon surface after 3 days without polarisation at 980 °C. a) compact layer covering interface, b) porous layer filled with bath and c) delaminating of carbide layers

3.2 Experiments with polarisation

3.2.1 Polarisation with a conventional cell

A conventional industrial electrolysis setup (Fig. 1b) was run for 35 min before being terminated due to a rapidly increasing cell voltage from 2.4 ± 0.2 V in the first 30 min. An optical micrograph and Al, C, Na, F element maps are shown in Fig. 5. An aluminium carbide layer of about 10 µm is observed at the carbon surface while a bath film is observed between the aluminium and carbon. The thickness of the carbide layer is relatively even over the whole cathode surface. However, the layer appears porous and polycrystalline with agglomerated carbide grains and several small gaps. The formation of aluminium carbide is clearly much faster during electrolysis compared to the purely chemical reaction rate.
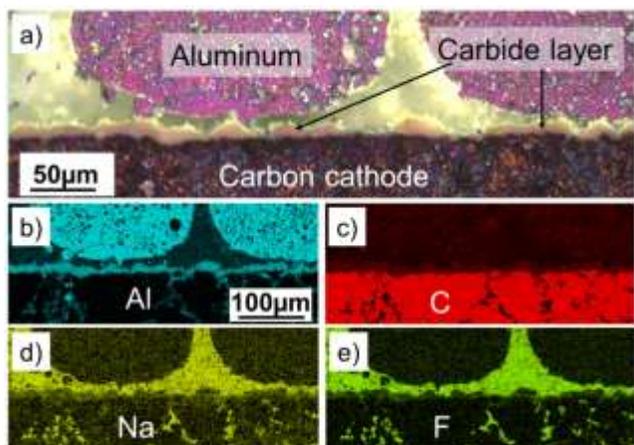
Fig. 5   Al/C interface after polarisation at 980 °C for 35 minutes. a) Polarised light image. b-f) Al, C, Na, F element maps
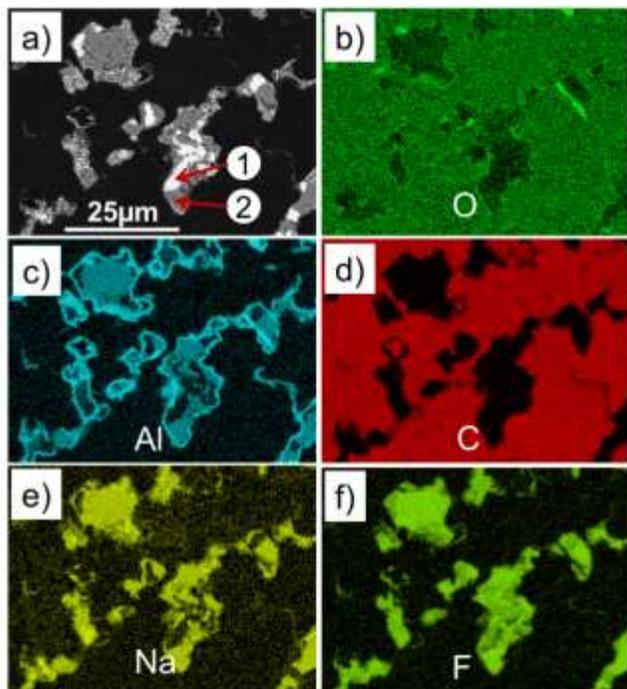
Fig. 6   Cathode after 35 min electrolysis in conventional cell setup. a) SEM image. b-f) O, Al, C, Na, F element maps

A SEM image and O, Al, C, Na, F element maps of the carbon cathode is shown in Fig. 6. The pores of the carbon cathode are filled with bath. Aluminium carbide is also observed to be formed on the walls as evidenced in the Al element map. No Al metal was detected in the interior of the carbon material. EDS point analysis of the bright and grey areas inside pores reveals that the bright area is CaF_2 rich. Compositions from the EDS analysis is listed in Table 1, showing that the frozen bath consists of CaF_2 and Na_3AlF_6.

Table 1   Composition (in at%) in point 1 and 2 in Fig. 6 determined by EDS.

	Na	Al	Ca	C	O	F	Total
1	1.1	0.2	33.7	6.3	0.1	58.6	100.0
2	24.7	9.6	0.6	13.4	0	51.6	100.0

3.3   Polarisation with an invert cell

3.3.1   Inverted cell with initial presence of aluminium

In the inverted cell (Fig. 1c), the cell voltage was relatively stable in the range 0.25-0.35 V. As expected, this voltage is much lower than observed in the conventional electrolysis cell as the Al acted as an anode. Increasing the current density to 1 A/cm^2 increased the cell voltage to about 1.3 V. Optical image and O, Al, C, Na, F element maps of the surface of the top carbon cathode in the inverted cell is shown in Fig. 7. Aluminium carbide is observed both at the surface and in the pores of the cathode. As aluminium was not intended to be in contact with the cathode and the observed aluminium in the bath close to the cathode is most likely cathodically deposited aluminium. Analysis of the interior of the cathode revealed the same result as in the conventional cell set-up (Fig. 6), with bath and aluminium carbide in the pores. The morphology of the carbide layer is comparable to the morphology of the carbide layer formed in the conventional cell.
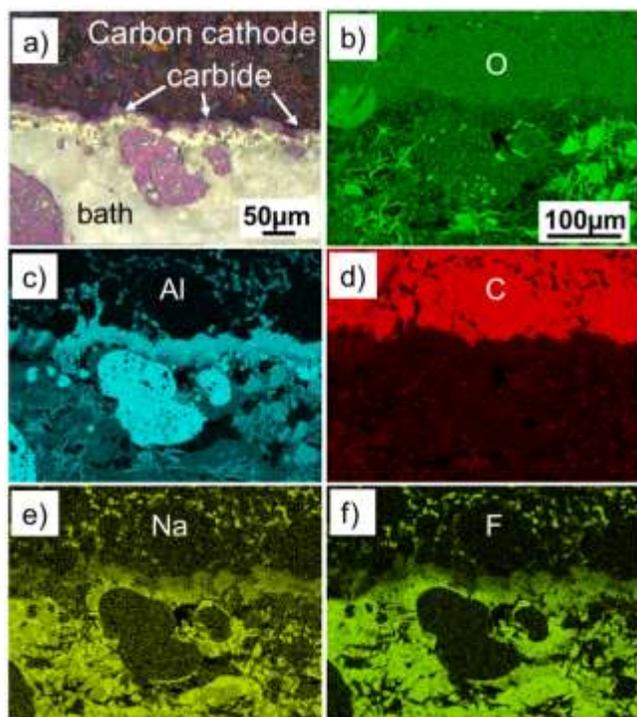
Fig. 7   Al/C interface after polarisation at 980 °C for 3 hours in inverted cell. a) Polarised light image. b-f) Al, C, Na, F element maps

3.3.2   Inverted cell without aluminium present initially

An experiment with an inverted cell without aluminium initially was also performed (Fig. 1d). The cell voltage (2.2 V) was similar to the voltage observed in the conventional cell. In this case the cell voltage started to increase first after about 60-80 minutes. Optical image and O, Al, C, Na, F element maps of the cathode interface are shown in Fig. 8. An aluminium carbide layer was also found on the carbon surface in this case, but the thickness was thinner compared to the conventional and the inverted cell with aluminium pad initially. The morphology of the carbide layer was similar to the other experiments with a porous layer and the cathode filled with bath and an aluminium carbide layer. The metallic aluminium formed at the cathode during electrolysis were only present close to the cathode surface. No aluminium was observed at the anode.
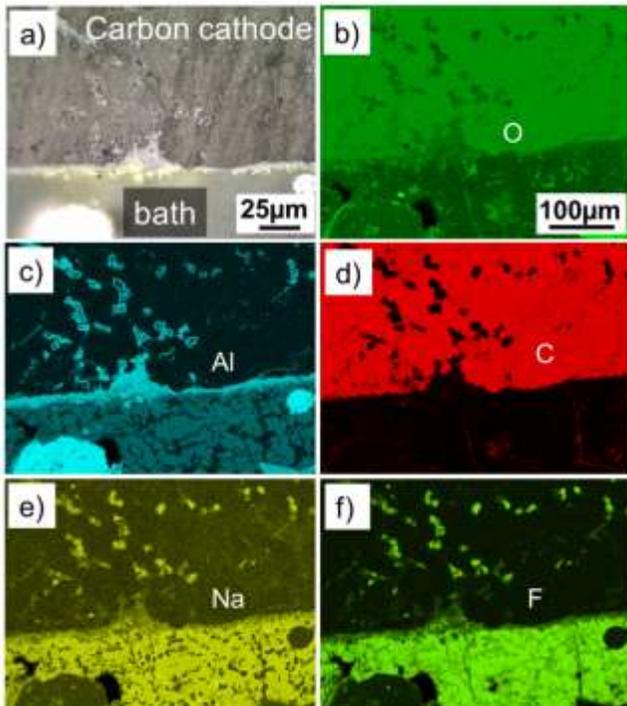
Fig. 8   Al/C interface after polarisation at 980 °C for 90 minutes in inverted cell with no initial Al pool. a) Polarised light image a). b-f) Al, C, Na, F element maps

2.3 Analysis of anode surfaces after polarisation tests

The surfaces of the anodes after the three electrolysis tests using b, c, and d setups shown in Fig. 1 were also analysed.
Fig. 9 shows the optical image and O, Al, C, Na, F element maps of the anode surface after 3 hours electrolysis in the inverted cell setup shown in Fig. 1c. The analysis confirmed that there was no aluminium carbide formed at the anode surface. However, the Al, Na, F element maps confirmed that the electrolyte had penetrated the pores of the anode in the inverted cell. It is not clear if the infiltration occurred during or after polarisation. The analysis of the anode surfaces from the other two polarisation tests showed quite similar patterns.

7
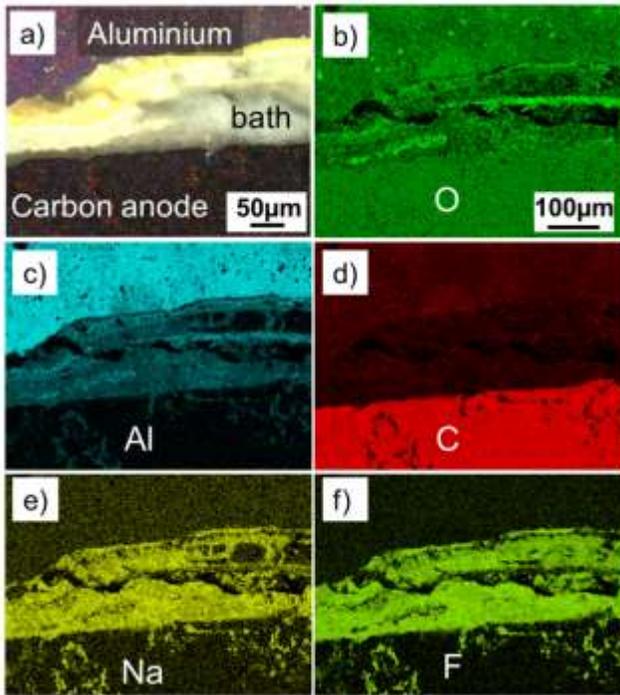
Fig. 9   Anode interface after polarisation at 980 °C for 3 hours in inverted cell. a) Polarised light image. b-f) Al, C, Na, F element maps

4   DISCUSSION

The experiments without polarisation of the electrodes showed that significant longer time was needed to form a carbide layer at the carbon surface through a chemical reaction between Al and C, Reaction 4

$$4\,Al(l) + 3\,C(s) \rightarrow Al_4C_3 \qquad (4)$$
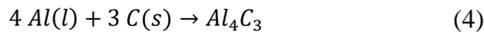
These results are in line with Grjotheim [8], which reported that formation of aluminium carbide due to Reaction 4 with dissolution of the carbide into the bath proceeds until saturation. The saturation time is dependent on several factors such as the amount and composition of the molten fluoride, aluminium-carbon contact interface and thermal convection in the bath during the experiment. Grjotheim also observed a strong correlation between the amount of carbide formed and the porosity of the carbon material. Hence, the formation of the aluminium carbide reflected the topography of the carbon material. Higher porosity gives larger surface area and results in increased aluminium carbide formation.

In the present experiments, an aluminium carbide layer was evident at the cathode after 35 minutes when a electrolysis setup similar to a conventional aluminium electrolysis cell was used. Electrochemical formation of aluminium carbide, according to Reaction 5, is therefore significantly faster compared to Reaction 4 with no current or polarisation of the electrodes.

$$4Al^{3+}(l) + 3C + 12e^- \rightarrow Al_4C_3 \qquad (5)$$
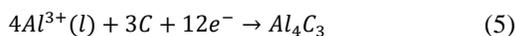
The morphology of the carbide layer was similar to the layer formed without electrochemical reactions, referred to as the chemical reaction in the following. All carbide layers were polycrystalline and porous, and the layers resemble similar carbide layers observed in industrial cells reported by Østrem [12]. Such morphology also fits with the hypothesis suggested by Solheim [13], where aluminium carbide layer acts as a current shield on the carbon cathode. Areas which are not covered with carbide should have significantly higher current densities and excessive wear, especially on the edges of these "carbide islands". However, in an industrial cell the carbide layer is changing over time due to the influence of hydrodynamics in the aluminium pad, the amount of bath near the cathode, sludge formation/removal, etc. The morphology of the layer is a result of the competition between formation of aluminium carbide and dissolution into the bath/pad. Faster formation and slower dissolution means carbide layer growth, but the formation is continuously slowed down as the layer grows, which reduce the current density through this region. This suggests that the areas which are not covered with aluminium carbide are dynamic. Stable cell voltage also suggests that carbide layer does not represent significant variation in the overall electrical resistivity in terms of the cell, but may play a role as a local current shield.

Analysis of the pores in the cathode suggests that carbide is formed by electrochemical deposition directly from the bath since carbide layer was observed on the walls, while no aluminium was found in the pores. The dominating electrochemical reaction may be different in the

pores relative to the outer surface of the cathode, however, the formation of aluminium carbide in the pores is a strong indication of a reaction between bath and carbon promoted by the conditions created during electrochemical polarisation.

It is challenging to evaluate the direct involvement of aluminium metal in the formation of aluminium carbide. In the areas with no contact between carbon and aluminium metal, the main cathodic reaction is aluminium deposition and the formation of aluminium carbide may proceed in two steps. The first step is aluminium deposition and second step is the chemical reaction between Al metal and carbon cathode. This mechanism is however not likely, because the second step, the direct chemical reaction, is shown to be slow.

Cell voltage during the electrolysis was more than 2 V for the conventional cell using setup shown in Fig. 1, and increased dramatically in the period from 30 to 35 min before the experiment was stopped. The overall electrolysis reaction is expressed by Reaction 6. The reversible voltage for alumina decomposition in the conventional cell by this reaction is 1.2 V. The remaining of the cell voltage is supposed to be the ohmic resistivity of the bath and of the other cell components. The cathodic overvoltage is usually small, while the anode overvoltage is likely to be larger except for the inverted cell with the aluminium pool.

$$2Al_2O_3 + 3C \rightarrow 4Al + 3CO_2 \qquad \text{E = 1.2 V} \qquad (6)$$
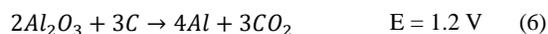
The calculation from Faraday's law confirmed that the amount of alumina introduced to the bath lasted for 35 min at prevailing electrolysis conditions and aluminium deposition is considered as the only reaction. It means there was negligible dissolution of alumina from the crucible, which may act as a source of alumina for the electrolysis.

Electrolysis in the inverted cell using setup shown in Figure 1c) had lower cell voltage, only 0.3 V compared to more than 2 V in the conventional cell setup mentioned above. There is no aluminium decomposition taking place, but only cyclic reduction and oxidation of aluminium which is expressed by Reactions 7. Reversible voltage of the inverted cell is 0 V and the measured cell voltage represents only the resistivity of the cell. The cathode reaction is the same as in the conventional cell, but on the anode there is no CO_2 evolution, only the oxidation of aluminium, which is in contact with the anode.

$$\begin{aligned} Al^{3+} + 3e^- &\rightarrow Al \\ Al &\rightarrow Al^{3+} + 3e^- \end{aligned} \qquad \text{E = 0 V} \qquad (7)$$

The cell voltage in the electrolysis without aluminium using setup shown in Fig. 1d was more than 2 V, which means that alumina decomposition was the main reaction. The overall electrolysis reaction was also Reaction 6. It might be expected that an aluminium pad is established on the anode after short time of electrolysis, which would then result into low cell voltage comparable to the inverted cell with aluminium present initially. However, this did not happen because the efficiency of the back reaction is expected to be high. Aluminium formed on the cathode at the top of the cell is falling down towards the anode bottom and at the same time, CO_2 formed on the anode bottom is moving upwards meeting the aluminium in the bulk of the bath and possibly also reaching the cathode surface. A schematic illustration is shown in Fig. 10.

The product of the back reaction, aluminium oxide, can undergo electrochemical decomposition and the forward reaction might proceed without additional alumina feeding longer than the time predicted by Faraday's law. The calculation from Faraday's law showed, however, that alumina added initially corresponds to ~90 min of electrolysis, which correlates well with the time when the cell voltage started to increase dramatically. That implies the aluminium oxide form by the back reaction does not contribute to the cathodic decomposition reaction. In this experiment, β-alumina were found in the bath close to the cathode surface. The formation of β-alumina might be an explanation why alumina formed by the back reaction does not undergo electrolysis, but accumulates in the bath. β-alumina is a polymorph of alumina containing significant amounts of sodium and the formation is therefore more likely in more basic electrolytes with higher cryolite ratio. Aluminium carbide layer with the same morphology was observed, but thinner compared to the conventional and the inverted cell with aluminium. This can be explained by faster dissolution of carbide to the bath, because the carbon surface was not protected by Al metal and there was also higher amount of bath in the vicinity of the cathode. Additionally, the stirring effect of the gas bubbles might have contributed.
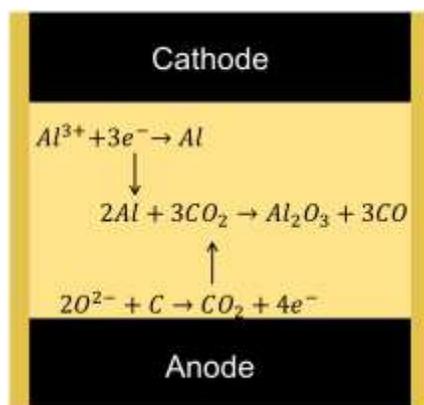
Fig. 10   Schematic illustration of electrode reactions and the back reaction during the electrolysis in inverted cell setup without aluminium present initially

Analysis of the anodes revealed that bath had also penetrated into this electrode, but aluminium carbide was not found on the carbon surface. Cryolite does not wet carbon very well (wetting angle around 90°), but when carbon is anodically polarised, the wetting properties are improving (wetting angle around 20°) [14]. When aluminium is in contact with carbon and cryolite is present, aluminium carbide can be formed without cathodic polarisation, but it is a slow process. This might be the case of inverted cell, where one might expect chemical formation of aluminium carbide. However, aluminium carbide undergoes oxidation on the anode by Reaction 8.

$$Al_4C_3 + 12NaF \rightarrow 4AlF_3 + 3C + 12Na^+ + 12e^- \qquad (8)$$
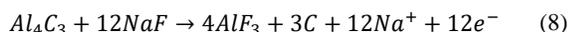
If regular carbon oxidation is the main anode reaction, aluminium carbide can be oxidized by anode gases, see Reaction 9.

$$Al_4C_3 + 6CO_2(g) \rightarrow Al_2O_3 + 3C + 6CO(g) \qquad\qquad (9)$$
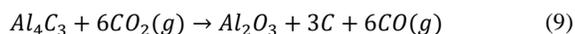
Anodic oxidation of carbide is a fast process and it explains why aluminium carbide could not be found on the anode.

Finally, it was not observed any significant differences in the microstructure of aluminium carbide layers in the various electrochemical cells. This suggests that the electrochemical formation of aluminium carbide involve the same species in the electrolyte.

5   CONCLUSIONS

Formation of layer of aluminium carbide by the direct chemical reaction between the elements was demonstrated after 3 days in the cell without electrolysis involved. Electrochemical formation of aluminium carbide was shown to be considerably faster compared to the chemical reaction, where aluminium carbide layer was observed already after 35 min of electrolysis. An aluminium carbide layer with similar morphology but thinner was also observed after electrolysis in the cell without aluminium present initially. Aluminium carbide was also shown to be formed on the walls of the pores in the cathode, but no aluminium metal was found to be formed inside the cathode. This suggests that aluminium carbide was deposited directly from the bath without involvement of aluminium metal. Formation of aluminium carbide in the invert cell without initial presence of aluminium also supports this mechanism. The morphology of the carbide layer was relatively similar in all the cells. Only the thickness was varying, which most likely depend on the kinetics of the dissolution into the bath, which is suggested as the rate determining step.

6   ACKNOWLEDGEMENTS

7   REFERENCES

1. Tschöpe K, Støre A, Skybakmoen E, Solheim A, Grande T, Ratvik AP (2013) Critical Reflections on Laboratory Wear Test for Ranking Commercial Cathode Materials in aluminium Cells, Light Metals 2013:1251-1256
2. Tschöpe K, Skybakmoen E, Solheim A, Grande T (2013) Cathode wear in Hall-Héroult cells, Aluminium 1-2: 40-43.
3. Tschöpe K, Støre A, Solheim A, Skybakmoen E, Grande T, Ratvik AP (2013) Electrochemical wear of carbon cathodes in electrowinning of aluminium, JOM 65(11): 1403-1410. doi: 10.1007/s11837-013-0605-4

4. Dorward RC (1973) Reaction between Aluminium and Graphite in the Presence of Cryolite, Met. Trans. 4(1): 386-388.
5. Novak B, Tschöpe K, Ratvik AP, Grande T (2012) Fundamentals of Aluminium Carbide Formation, Light Metals 2012: 1343-1348.
6. Novak B, Tschöpe K, Ratvik AP, Grande T (2013) The effect of Cryolite on the Formation of Aluminium Carbide at the Carbon Aluminium Interface, Light Metals 2013:1245-1250
7. Landry K, Kalogeropoulou S, Eustathopoulos N (1998) Wettability of Carbon by Aluminium in Aluminium Alloys, Mater. Sci. Eng. A254: 99-111
8. Grjotheim K, Næumann R, Øye HA (1977) Formation of Aluminium Carbide in the Presence of Cryolite Melts, Light Metals 1977: 233-242
9. Skybakmoen E, Rørvik S, Solheim A, Holm KR, Tiefenbach P, Østrem Ø (2011) Measurement of Cathode Surface Wear Profiles by Laser Scanning, Light Metals 2011:1061-1066.
10. Liao X, Øye HA (1999) Carbon Cathode Corrosion by Aluminium Carbide Formation in Cryolitic Melts, Light Metals 1999: 621-627
11. Tschöpe K, Støre A, Rørvik S, Solheim A, Skybakmoen E, Grande T, Ratvik AP (2012) Investigation of the Cathode Wear Mechanism in a Laboratory Test Cell, Light Metals 2012: 1349-1354
12. Østrem Ø (2013) Cathode Wear in Hall-Héroult Cells, PhD Thesis, NTNU, Trondheim, February 2013, pp. 89-112
13. Solheim A, Tschöpe K (2013) Model for Excessive Cathode Wear by a "Carbon Pump" at the Cell Bottom, Light Metals 2013: 1257-1262.
14. Qui ZX, Wei QB, You KT (1983) Studies on wettability of carbon electrodes in aluminium electrolysis. Pt. 1, Aluminium 59(9): 670-673